Scientia Iranica B (2014) 21(6), 1896–1906

SCIENTIA IRANICA

Sharif University of Technology
Scientia Iranica
Transactions B: Mechanical Engineering
www.scientiairanica.com

Vibration and buckling analysis of functionally graded beams using reproducing kernel particle method

R. Saljooghi[a], M.T. Ahmadian[a,b,*] and G.H. Farrahi[a]

a. *School of Mechanical Engineering, Sharif University of Technology, Tehran, Iran.*
b. *Center of Excellence in Design, Robotics and Automation (CEDRA), Sharif University of Technology, Tehran, Iran.*

Received 7 October 2012; received in revised form 21 December 2013; accepted 9 March 2014

KEYWORDS
Functionally graded beam;
Reproducing kernel particle method;
Natural frequencies;
Critical buckling loads.

Abstract. This paper presents the vibration and buckling analysis of functionally graded beams with different boundary conditions, using the Reproducing Kernel Particle Method (RKPM). Vibration of simple Euler-Bernoulli beams using RKPM is already developed and reported in the literature. So far, the modeling of FGM beams using the theoretical method or the finite element technique has not evolved with accurate results for the power law form of FGM with a large power of "n" value. The accuracy of RKPM results is very good and is not sensitive to the n value. The system of equations of motion is derived using Lagrange's method under the assumption of the Euler-Bernoulli beam theory. Boundary conditions of the beam are taken into account using Lagrange multipliers. It is assumed that material properties of the beam vary continuously in the thickness direction, according to the power-law form. RKPM is implemented to obtain the equation of motion and, consequently, natural frequencies and buckling loads of the FGM beam are evaluated. Results are verified for special cases reported in the literature. Considering the displacement of the neutral axis, buckling loads, with respect to length and material distribution, are evaluated. For special cases of homogenous beams, RKPM matches theoretical evaluation with less than one percent error.

1. Introduction

One of the new concepts in material design is the concept of Functionally Graded Materials (FGM). These materials are mostly made of ceramic and metallic components, with properties varying from one side to the other, in the form of a particular distribution function. This enables FGM structures to be flexible for any desired properties. The exclusive characteristic of functionally graded materials is the continuous and smooth change in properties, which reduces undesirable phenomena, such as stress concentration. Functionally graded materials are used to make gradual changes in the mechanical properties and characteristics of structures [1].

FGMs are of interest for a wide range of applications, such as artificial teeth and dental implants, sensors, biomedicine, different aspects of tissue engineering and aerospace industries [2-8]. The idea of combining two different types of material was introduced by Bever and Duwez in 1972 [9]. Over the last decades, many studies have been devoted to understanding the static and dynamic behavior of these materials. Due to the continuous change of properties, analysis of FGMs results in mathematical complications, applying analytical solution to which becomes difficult. Considering the application of beams in most structures, studying the vibration and mechanical performance of FGM beams is of great importance. Chakraborty et

*. *Corresponding author. Tel.: +98 21 66165503*
E-mail addresses: saljooghi.reza@gmail.com (R. Saljooghi); ahmadian@sharif.edu (M.T. Ahmadian); farrahi@sharif.edu (G.H. Farrahi)

al. [10] developed a new beam finite element for the analysis of functionally graded materials. They used the exact solution of the static part of the governing differential equations to construct interpolating polynomials for the element formulation, and showed the behavioral difference of functionally graded material beams with pure metal or pure ceramic beams for both exponential and power-law variations of material properties. Xiang and Yang [11] investigated the free and forced vibration of a laminated functionally graded beam of variable thickness under thermally induced initial stresses within the framework of the Timoshenko beam theory. The beam consisted of a homogeneous substrate and two heterogeneous functionally graded layers whose material composition followed a power law distribution in the thickness direction. It was assumed that the beam might be clamped, hinged, or free at its ends. They showed that vibration frequencies, mode shapes and dynamic responses of the beam, were significantly influenced by thickness variation, temperature change, slenderness ratio and end support conditions. Aydogdu [12] analyzed the vibration and buckling of simply supported axially FGM beams using the semi-inverse method, assuming the Euler-Bernoulli beam theory. Simsek and Kocatürk [13] investigated free vibration characteristics and dynamic behavior of a functionally graded simply supported beam under a concentrated moving harmonic load. The system of equations of motion was derived using Lagrange's equations under the assumption of the Euler-Bernoulli beam theory, and the constraint conditions of supports were taken into account using Lagrange multipliers. They discussed the effects of different material distribution, the velocity of the moving harmonic load and excitation frequency on the dynamic response of the beam. Sina et al. [14] used a new beam theory, different from the traditional first-order shear deformation beam theory, to analyze free vibration of functionally graded beams. The equations of motion were derived using Hamilton's principle and solved using an analytical method. The effects of boundary conditions, volume fraction and shear deformation on natural frequencies and mode shapes were investigated. Simsek [15] investigated vibration of a functionally graded simply-supported beam under a moving mass using different beam theories. The material properties of the beam varied continuously in the thickness direction, according to the power law form. The system of equations of motion were derived using Lagrange's equations, while the constraint conditions of supports were taken into account using Lagrange multipliers. The effects of shear deformation, various material distributions, velocity of the moving mass, inertia, Coriolis and the centripetal effects of the moving mass, on the dynamic displacements and stresses of the beam were discussed and compared with those of previous literature. Alshorbagy et al. [16] presented the dynamic characteristics of functionally graded beams with material graduation in axial or transversal directions, based on the power law form. They derived a system of equations of motion using the principle of virtual work and the finite element method to discretize the model. Effects of different material distribution, slenderness ratios, and boundary conditions, on the dynamic characteristics of the beam, are discussed.

The purpose of this paper is to evaluate vibration frequencies and buckling loads of functionally graded beams using the RKPM meshless method. The system of equations of motion is derived using Lagrange's method within the framework of the Euler-Bernoulli beam theory. Boundary conditions of supports are taken into account using Lagrange multipliers. It is assumed that the material properties of the beam vary continuously in the thickness direction, according to the power law form.

2. Theory and formulation

Figure 1 shows an FGM beam with length, L, and thickness, h. A schematic of the beam cross section under bending moment, $M\frown$, with the assumption of the Euler-Bernoulli beam theory, is presented in Figure 2. The normal strain in an arbitrary point in the thickness of the beam is given by [17]:

$$\varepsilon_{xx} = \frac{\partial u}{\partial x}. \tag{1}$$

The displacement field of the beam may be written as:

$$w = w, \qquad u = -z\frac{\partial w}{\partial x}, \qquad v = 0, \tag{2}$$

where w, u and v are transverse, axial and lateral displacements of any point of the beam, respectively. Substituting Eq. (2) into Eq. (1) yields:

$$\varepsilon_{xx} = \frac{\partial u}{\partial x} = -z\frac{\partial^2 w}{\partial x^2}. \tag{3}$$

The stress field in the xx plane is [14]:

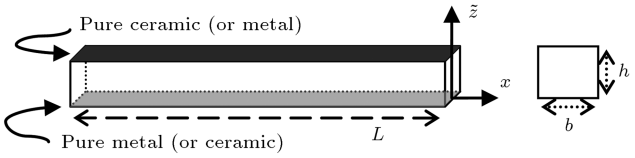

Figure 1. A functionally graded beam.

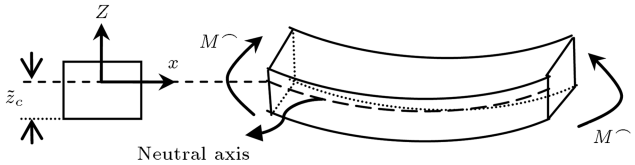

Figure 2. An FGM beam under bending moment.

$$\sigma_{xx} = E(\tilde{z})\varepsilon_{xx} = -E(\tilde{z})z\frac{\partial^2 w}{\partial x^2}, \tag{4}$$

where $E(\tilde{z})$ is the Young modulus of the beam. The potential energy of the beam can be written as [17]:

$$U = \frac{1}{2}\int_0^L \int_A \varepsilon_{xx}\sigma_{xx} dA dx, \tag{5}$$

where A is the cross section of the beam. Substituting Eqs. (3) and (4) into Eq. (5) yields:

$$U = \frac{1}{2}\int_0^L \int_A E(\tilde{z})z^2 \left(\frac{\partial^2 w}{\partial x^2}\right)^2 dA dx. \tag{6}$$

For a homogeneous beam, potential energy is [17]:

$$U = \frac{1}{2}\int_0^L EI \left(\frac{\partial^2 w}{\partial x^2}\right)^2 dx, \tag{7}$$

in which, I is the moment of inertia of the beam cross-section. Comparing Eqs. (6) and (7) without loss of generality, an equivalent EI for the FGM beam can be introduced as:

$$(EI)_{\text{eq}} = \int_A z^2 E(\tilde{z}) dA. \tag{8}$$

For any arbitrary distribution of materials, the location of the neutral axis may be evaluated as follows [18]:

$$\tilde{z}_c = \frac{\int_A E(\tilde{z})\tilde{z} dA}{\int_A E(\tilde{z}) dA}. \tag{9}$$

Having the position of the neutral axis, according to Figure 1, the equivalent EI for the FGM beam will be:

$$(EI)_{\text{eq}} = \int_0^h (\tilde{z} - \tilde{z}_c)^2 E(\tilde{z}) b d\tilde{z}. \tag{10}$$

The kinetic energy of the beam for transverse vibration is [17]:

$$T = \frac{1}{2}\int_0^L m \left(\frac{\partial w}{\partial t}\right)^2 dx, \tag{11}$$

in which m is the mass per unit length of the beam and is obtained as below:

$$m = \int_A \rho(\tilde{z}) dA = \int_0^h \rho(\tilde{z}) b d\tilde{z}, \tag{12}$$

where $\rho(\tilde{z})$ is the density of the FGM beam.

In Eqs. (4) to (12), material properties of the FGM beam vary continuously in the thickness direction according to the power law form:

$$\rho(\tilde{z}) = \rho_b + \left(\frac{\tilde{z}}{h}\right)^n (\rho_t - \rho_b),$$

$$E(\tilde{z}) = E_b + \left(\frac{\tilde{z}}{h}\right)^n (E_t - E_b), \tag{13}$$

where subscripts, t and b, refer to top and bottom. From Eqs. (6) and (11), using Lagrange's theorem, the equation of the transverse vibration of the FGM beam is obtained as below:

$$(EI)_{\text{eq}}\frac{\partial^4 w(x,t)}{\partial x^4} + m\frac{\partial^2 w(x,t)}{\partial t^2} = 0. \tag{14}$$

To solve Eq. (14), $w(x,t)$ is reproduced using RKPM shape functions, and natural frequencies are obtained from the eigenvalue equation.

3. Overview of RKPM

The reproduced function in RKPM is [19]:

$$u^R(x) = \int_\Omega \overline{\phi}_a(x; x-y)u(y)dy, \tag{15}$$

in which, $\overline{\phi}$ is the corrected kernel function defined as:

$$\overline{\phi}_a(x; x-y) = C(x; x-y)\phi_a(x-y), \tag{16}$$

where C is the correction function and ϕ_a is kernel function:

$$C(x; x-y) = \sum_{i=0}^n b_i(x)(x-y)^i = b^T H(x-y),$$

$$H^T(x-y) = \begin{bmatrix} 1 & x-y & (x-y)^2 & \cdots & (x-y)^n \end{bmatrix},$$

$$\phi_a(x-y) = \frac{1}{a}\phi\left(\frac{x-y}{a}\right). \tag{17}$$

Defining the moments of kernel function in the following form:

$$m_k(x) = \int_\Omega (x-y)^k \phi_a(x-y)dy, \tag{18}$$

the Taylor series expansion of $u(y)$ can be expressed as below:

$$u(y) \cong \sum_{a=0}^n \left[\frac{(-1)^a(x-y)^a}{a!}u^{(a)}(x)\sum_{i=0}^n b_i(x)m_{a+i}(x)\right]. \tag{19}$$

In order for the reproduced function to be equal to the main function, the following conditions must be

satisfied:

$$\sum_{i=0}^{n} b_i(x)m_i(x) = 1,$$

$$\sum_{i=0}^{n} b_i(x)m_{a+i}(x) = 0, \qquad a = 1, 2, \cdots, n. \tag{20}$$

Eq. (20) can be written in the matrix form:

$$\widetilde{M}(x)b(x) = H(0), \tag{21}$$

in which matrix $\widetilde{M}$ is:

$$\begin{bmatrix} m_0 & m_1 & \cdots & m_n \\ m_1 & m_2 & \cdots & m_{n+1} \\ \vdots & \vdots & \ddots & \vdots \\ m_n & m_{n+1} & \cdots & m_{2n} \end{bmatrix}. \tag{22}$$

By solving the matrix Eq. (21), unknown coefficients, $b_i(x)$ and the eventually reproduced function, $u^R(x)$ are obtained.

Applying the trapezoidal rule to Eq. (15) leads to the discretized form of RKPM:

$$u^R(x) = \sum_{I=1}^{NP} \psi_I(x)u(x_I), \tag{23}$$

where:

$$\psi_I(x) = \left[\sum_{i=1}^{n} b_i(x)(x - x_I)^i\right] \phi_a(x - x_I)\Delta x_I,$$

is the shape function of particle I, $u(x_I)$ is the parameter associated with particle I, NP is the total number of particles and Δx_I is the specific length of particle I.

$$\Delta x_I = \begin{bmatrix} \frac{x_2 - x_1}{2} & I = 1 \\ \frac{x_{I+1} - x_{I-1}}{2} & I = 2, \cdots, \mathrm{NP} - 1 \\ \frac{x_{\mathrm{NP}} - x_{\mathrm{NP}-1}}{2} & I = \mathrm{NP} \end{bmatrix}. \tag{24}$$

4. RKPM for free vibration analysis of FGM beams

Similar to the method used in [20,21], using Lagrange multipliers to impose boundary conditions in the weak form of Eq. (14) at different end supports leads to the following equations:

(a) Simply-simply supported:

$$\int_0^l \frac{\partial^2 w}{\partial x^2}\frac{\partial^2 \delta w}{\partial x^2}dx + \frac{m}{EI_{\mathrm{eq}}}\int_0^l \frac{\partial^2 w}{\partial t^2}\delta w dx + \frac{\partial^3 w}{\partial x^3}\delta w\Big|_0^l + \delta\ \frac{\partial^3 w}{\partial x^3}w\Big|_0^l = 0. \tag{25}$$

(b) Clamped-simply supported:

$$\int_0^l \frac{\partial^2 w}{\partial x^2}\frac{\partial^2 \delta w}{\partial x^2}dx + \frac{m}{EI_{\mathrm{eq}}}\int_0^l \frac{\partial^2 w}{\partial t^2}\delta w dx + \frac{\partial^3 w}{\partial x^3}\delta w\Big|_0^l + \delta\ \frac{\partial^3 w}{\partial x^3}w\Big|_0^l + \frac{\partial^2 w}{\partial x^2}\delta\frac{\partial w}{\partial x}\Big|_0 + \delta\ \frac{\partial^2 w}{\partial x^2}\frac{\partial w}{\partial x}\Big|_0 = 0. \tag{26}$$

(c) Clamped- free:

$$\int_0^l \frac{\partial^2 w}{\partial x^2}\frac{\partial^2 \delta w}{\partial x^2}dx + \frac{m}{EI_{\mathrm{eq}}}\int_0^l \frac{\partial^2 w}{\partial t^2}\delta w dx - \frac{\partial^3 w}{\partial x^3}\delta w\Big|_0 - \delta\ \frac{\partial^3 w}{\partial x^3}w\Big|_0 + \frac{\partial^2 w}{\partial x^2}\delta\frac{\partial w}{\partial x}\Big|_0 + \delta\ \frac{\partial^2 w}{\partial x^2}\frac{\partial w}{\partial x}\Big|_0 = 0. \tag{27}$$

(d) Clamped-clamped:

$$\int_0^l \frac{\partial^2 w}{\partial x^2}\frac{\partial^2 \delta w}{\partial x^2}dx + \frac{m}{EI_{\mathrm{eq}}}\int_0^l \frac{\partial^2 w}{\partial t^2}\delta w dx + \frac{\partial^3 w}{\partial x^3}\delta w\Big|_0^l + \delta\ \frac{\partial^3 w}{\partial x^3}w\Big|_0^l - \frac{\partial^2 w}{\partial x^2}\delta\frac{\partial w}{\partial x}\Big|_0^l - \delta\ \frac{\partial^2 w}{\partial x^2}\frac{\partial w}{\partial x}\Big|_0^l = 0. \tag{28}$$

Applying RKPM discretization to the above weak forms leads to stiffness and mass matrices. w and δw can be expressed in the form of Eq. (23):

$$w(x,t) = \sum_{I=1}^{\mathrm{NP}} \Psi_I(x)D_I(t),$$

$$\delta w(x,t) = \sum_{I=1}^{\mathrm{NP}} \Psi_I(x)C_I(t), \tag{29}$$

where $D_I(t)$ and $C_I(t)$ are degrees of freedom for trial and test functions and assumed as:

$$D_I(t) = d_I e^{i\omega t},$$

$$C_I(t) = c_I e^{i\omega t}. \tag{30}$$

Finally, the vibration equation of the FGM beam is obtained as an eigenvalue matrix problem:

$$([K] - \omega_i^2[M])\{\Phi_i\} = 0, \tag{31}$$

where ω_i and Φ_i are the natural frequency and mode shape of the beam.

For example, discretization for a simply-simply supported beam leads to the stiffness and mass matrices as below:

$$M_{ij} = \int_0^l \frac{m}{EI_{\text{eq}}} \psi_i(x)^T \psi_j(x) dx,$$

$$K_{ij} = \int_0^l \frac{\partial^2 \psi_i(x)^T}{\partial x^2} \frac{\partial^2 \psi_j(x)}{\partial x^2} dx + \frac{\partial^3 \psi_i(x)^T}{\partial x^3} \psi_j(x) \Big|_0^l + \psi_i(x)^T \frac{\partial^3 \psi_j(x)}{\partial x^3} \Big|_0^l. \quad (32)$$

For numeric calculations, integrals of Eq. (32) are discretized using the trapezoidal rule.

5. Buckling of FGM beam

Using $(EI)_{\text{eq}}$, the general equation for transverse vibrations of an FGM beam under axial compression (Figure 3) can be written in a similar manner to a simple beam [19,20]:

$$(EI)_{\text{eq}} \frac{\partial^4 w(x,t)}{\partial x^4} + m \frac{\partial^2 w(x,t)}{\partial t^2} + p \frac{\partial^2 w(x,t)}{\partial x^2} = 0, \quad (33)$$

where p is the compressive axial load, which is positive in compression.

It should be noted that load, p, must be applied on the displaced neutral axis, otherwise the buckling analysis of FGM beams would be incorrect.

Using Lagrange multipliers to impose boundary conditions on the weak form of Eq. (33) for different end supports, under axial compression, leads to the following equations:

(a) Simply-simply supported:

$$EI_{\text{eq}} \int_0^l \frac{\partial^2 w}{\partial x^2} \frac{\partial^2 \delta w}{\partial x^2} dx + m \int_0^l \frac{\partial^2 w}{\partial t^2} \delta w dx - p \int_0^l \frac{\partial w}{\partial x} \delta w dx + \left(EI_{\text{eq}} \frac{\partial^3 w}{\partial x^3} + p \frac{\partial w}{\partial x} \right) \delta w \Big|_0^l + \left(EI_{eq} \delta \frac{\partial^3 w}{\partial x^3} + p \delta \frac{\partial w}{\partial x} \right) w \Big|_0^l = 0. \quad (34)$$

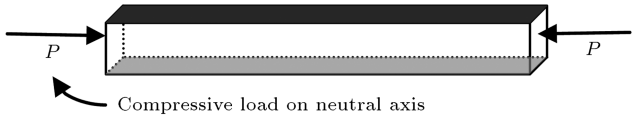

Figure 3. Beam under axial compression.

(b) Clamped-simply supported:

$$EI_{\text{eq}} \int_0^l \frac{\partial^2 w}{\partial x^2} \frac{\partial^2 \delta w}{\partial x^2} dx + m \int_0^l \frac{\partial^2 w}{\partial t^2} \delta w dx - p \int_0^l \frac{\partial w}{\partial x} \delta w dx + \left(EI_{\text{eq}} \frac{\partial^3 w}{\partial x^3} + p \frac{\partial w}{\partial x} \right) \delta w \Big|_0^l + \left(EI_{\text{eq}} \delta \frac{\partial^3 w}{\partial x^3} + p \delta \frac{\partial w}{\partial x} \right) w \Big|_0^l + EI_{\text{eq}} \frac{\partial^2 w}{\partial x^2} \delta \frac{\partial w}{\partial x} \Big|_0 + EI_{\text{eq}} \delta \frac{\partial^2 w}{\partial x^2} \frac{\partial w}{\partial x} \Big|_0 = 0. \quad (35)$$

(c) Clamped-free:

$$EI_{\text{eq}} \int_0^l \frac{\partial^2 w}{\partial x^2} \frac{\partial^2 \delta w}{\partial x^2} dx + m \int_0^l \frac{\partial^2 w}{\partial t^2} \delta w dx - p \int_0^l \frac{\partial w}{\partial x} \delta w dx - \left(EI_{\text{eq}} \frac{\partial^3 w}{\partial x^3} + p \frac{\partial w}{\partial x} \right) \delta w \Big|_0 - \left(EI_{\text{eq}} \delta \frac{\partial^3 w}{\partial x^3} + p \delta \frac{\partial w}{\partial x} \right) w \Big|_0 + EI_{\text{eq}} \frac{\partial^2 w}{\partial x^2} \delta \frac{\partial w}{\partial x} \Big|_0 + EI_{\text{eq}} \delta \frac{\partial^2 w}{\partial x^2} \frac{\partial w}{\partial x} \Big|_0 = 0. \quad (36)$$

(d) Clamped-clamped:

$$EI_{\text{eq}} \int_0^l \frac{\partial^2 w}{\partial x^2} \frac{\partial^2 \delta w}{\partial x^2} dx + m \int_0^l \frac{\partial^2 w}{\partial t^2} \delta w dx - p \int_0^l \frac{\partial w}{\partial x} \delta w dx + \left(EI_{\text{eq}} \frac{\partial^3 w}{\partial x^3} + p \frac{\partial w}{\partial x} \right) \delta w \Big|_0^l + \left(EI_{\text{eq}} \delta \frac{\partial^3 w}{\partial x^3} + p \delta \frac{\partial w}{\partial x} \right) w \Big|_0^l - EI_{\text{eq}} \frac{\partial^2 w}{\partial x^2} \delta \frac{\partial w}{\partial x} \Big|_0^l - EI_{\text{eq}} \delta \frac{\partial^2 w}{\partial x^2} \frac{\partial w}{\partial x} \Big|_0^l = 0. \quad (37)$$

Considering Eqs. (29)-(31), in a similar manner, stiffness and mass matrices are obtained. Solving the eigenvalue problem for the buckling of a FGM beam, results in natural frequencies and critical buckling loads.

6. Numerical results

This section is devoted to examples of the free vibration analysis of FGM beams with different materials and end supports. The order of the correction polynomial is considered 2 (n in Eq. (17) = 2) and the dilation parameter is considered 3.5 times the specific length of particle I ($a = 3.5\Delta x_I$). The number of particles is assumed to be 100, which are distributed evenly along the beam. This number of particles is selected after performing the convergence test. For the particular problems involved in this paper, 100 particles are enough to give very good results in comparison with theoretical findings for special cases. As the number of particles goes beyond this number in the actual problem, even though the computational time increases rapidly, no sensible change is achieved. To solve the equations of motion, several MATLAB codes are developed in 1D space and the results are presented in both tabular and graphical forms.

Example 1. Consider an FGM beam made of aluminum and alumina, as metal and ceramic, respectively, with properties varying according to the power-law given by Eq. (13). The bottom surface of the beam is pure alumina, whereas the top surface is pure aluminum. The properties of these materials are given in Table 1. Boundary conditions are assumed to be clamped-free.

Non-dimensional natural frequency maybe defined as [18]:

$$\lambda = \omega \sqrt{\frac{12\rho_b L^4}{E_b h^2}}. \tag{38}$$

To validate the present formulation for an FGM beam, a comparison is made between the results of RKPM and the analytical method [17] for the clamped-free boundary conditions in Table 2. From Eq. (13), as $n \to \infty$, the beam approaches a homogenous one. For $n = 10^6$, non-dimensional natural frequencies obtained from Eqs. (31) and (38) are compared with the homogenous beam [17]. Results reveal very good agreement, with a maximum difference of 0.85 percent. To validate the claim that 100 particles are enough to give very good results, the L_2-error norm of the first four non-dimensional natural frequencies obtained from RKPM, in the case of a homogenous beam, for which exact solutions are available, is presented in Figure 4. It is seen from this figure, as the number of particles goes beyond 100, even though the error decreases slightly, the computational time grows rapidly. Figure 5 shows variations of first and second non-dimensional natural frequencies versus the power exponent of Eq. (13). It is seen that increasing the power exponent leads to higher frequencies. By increasing the power exponent, properties of the FGM beam approach those of the

Table 1. Metal and ceramic properties.

Properties	Unit	Aluminum	Alumina
Elasticity modulus (E)	GPa	67	393
Density (ρ)	kg/m^3	2800	3960

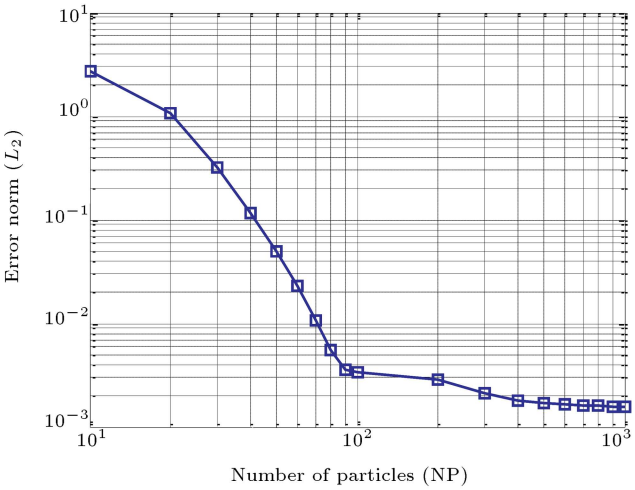

Figure 4. L_2-error norm of first four non-dimensional natural frequencies.

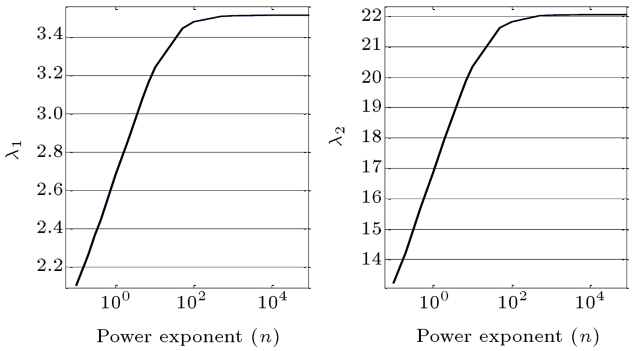

Figure 5. Variation of the first and second non-dimensional frequencies with the power-law exponent (n).

Table 2. Non-dimensional natural frequencies for homogenous beam.

Mode number	1	2	3	4
Ref. [17]	3.5160	22.034	61.696	120.903
RKPM with 21 particles	3.5152	22.061	61.973	121.951
RKPM with 51 particles	3.5158	22.033	61.703	120.930
RKPM with 101 particles	3.5159	22.034	61.695	120.901

material at the bottom surface. Since, in this example, the bottom surface is ceramic, the beam gets stiffer and natural frequencies increase. Table 3 represents first, second, and third natural frequencies for FGM beams with different material distributions. As mentioned before, when the power exponent (n) increases, the beam deviates from pure aluminum to pure alumina, which causes an increase in non-dimensional natural frequencies.

Example 2. Consider an FGM beam made of steel and alumina, as metal and ceramic, with material properties varying continuously in the thickness direction, according to the power law presented by Eq. (13). The bottom surface of the beam is assumed to be pure steel, whereas the top surface is pure alumina. Material properties of steel and alumina are given in Table 4. Considering the formulation used in Ref. [16] for non-dimensional natural frequency, i.e. $\lambda^2 = \omega\sqrt{12\rho_b L^4/E_b h^2}$, using RKPM, non-dimensional natural frequencies of the simply-simply supported beam are evaluated and represented in Table 5. In this table, the results for non-dimensional natural frequencies of the FGM beam, using the finite element technique [16], are also shown. Comparing the results of RKPM with the findings of Ref. [16] indicates a very good agreement. Figure 6 shows variations of the first and second non-dimensional natural frequencies, with respect to the power exponent of Eq. (13). It can be seen that, as the power exponent increases, natural frequencies tend to decrease. This is due to a reduction in the beam modulus of elasticity. Figure 7 presents variations of the first non-dimensional natural frequency of the FGM beam versus the power exponent, at different end supports. From this figure, it is clear that clamped-clamped support (cc) leads to the highest frequencies, where the lowest are obtained for clamped-free boundary conditions (cf). The first three non-dimensional natural frequencies for different boundary conditions and power exponents are given in Table 6. It is seen that as the power exponent increases, natural frequencies decrease. This is due to the fact that the structure changes from pure alumina to pure steel.

Table 3. Non-dimensional natural frequencies of FGM beam.

λ_i	$n=0$	$n=2$	$n=5$	$n=10$
λ_1	1.785	2.853	3.084	3.24
λ_2	11.031	19.90	19.35	20.33
λ_3	30.99	50.30	54.37	57.11

Table 4. Metal and ceramic properties.

Properties	Unit	Steel	Alumina
Elasticity modulus (E)	GPa	210	393
Density (ρ)	kg/m^3	7800	3960

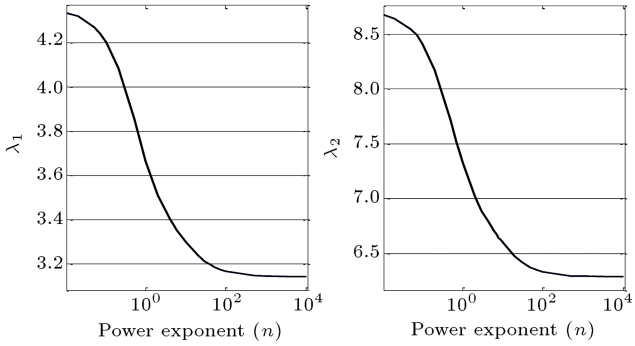

Figure 6. Variation of the first and second non-dimensional frequencies with the power-law exponent (n).

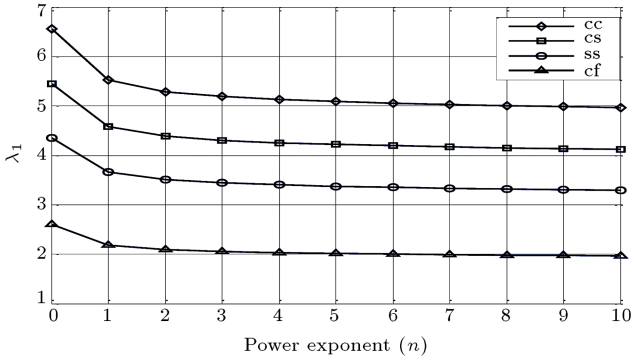

Figure 7. Variation of the first non-dimensional frequency with the power-law exponent (n) for different end supports.

Table 5. The first five non-dimensional frequencies for different material distribution.

	$n=0.2$		$n=2$		$n=10$	
	RKPM	Ref. [16]	RKPM	Ref. [16]	RKPM	Ref. [16]
λ_1	4.1781	4.2315	3.8014	3.9684	3.7031	3.8572
λ_2	8.2871	8.4500	7.6317	7.9245	7.3347	7.7026
λ_3	12.475	12.643	11.388	11.856	11.015	11.525
λ_4	16.325	16.798	15.233	15.752	14.817	15.312
λ_5	20.389	20.904	19.016	19.599	18.126	19.054

Table 6. The first three non-dimensional frequencies for different material distributions and different boundary conditions.

λ_i	BCs	$n = 0$	$n = 0.1$	$n = 0.5$	$n = 1$	$n = 5$	$n = 10^6$
λ_1	cf	2.593	2.503	2.297	2.183	2.012	1.875
	ff	0.000	0.000	0.000	0.000	0.000	0.000
	ss	4.344	4.215	4.025	3.995	3.871	3.141
	cs	5.430	5.242	4.810	4.572	4.214	3.926
	cc	6.541	6.315	5.795	5.507	5.076	4.729
λ_2	cf	6.491	6.267	5.751	5.465	5.073	4.694
	ff	6.541	6.315	5.795	5.507	5.076	4.730
	ss	8.689	8.388	8.102	7.921	7.554	6.283
	cs	9.775	9.438	8.660	8.230	7.585	7.068
	cc	10.86	10.485	9.621	9.144	8.427	7.853
λ_3	cf	10.862	10.491	9.632	9.172	8.431	7.864
	ff	10.860	10.484	9.621	9.144	8.427	7.853
	ss	13.034	12.583	12.021	11.685	11.215	9.425
	cs	14.120	13.632	12.509	11.889	10.957	10.21
	cc	15.206	14.680	13.472	12.803	11.800	10.995

Table 7. Critical buckling loads for a homogeneous simply-simply supported beam.

	$L = 2$ m	$L = 5$ m	$L = 10$ m
Analytical $\left(P_{cr} = \pi^2 \frac{EI}{L^2}\right)$	16.1615 MN	2.5858 MN	0.6465 MN
RKPM	16.1754 MN	2.5881 MN	0.6470 MN

7. Example of buckling

This section is devoted to the buckling analysis of an FGM beam under different boundary conditions and material distributions. For convenience, the beam of the second example is selected. According to the weak forms of the equation of motion of the beam with different boundary conditions (Eqs. (34)-(37)), the higher the compressive load p, the less the elements of stiffness matrix, resulting in the reduction of natural frequencies. As p increases, the first natural frequency tends to zero and buckling takes place. The p value, at which the first natural frequency becomes zero, is called the critical buckling load [22]. Using RKPM to solve the eigenvalue problem of the FGM beam, buckling loads can be obtained. To validate the present analysis for the buckling of an FGM beam, a comparison is made between results of RKPM and the analytical method [23]. Considering Eq. (13) as $n \to \infty$, the beam approaches a homogenous one, e.g. for $n = 10^6$ and critical buckling loads obtained from RKPM are compared with those of the analytical method for a homogenous beam (Table 7). The beam is considered to be made of alumina with simply supported boundary conditions, width of $b = 0.2$ m, thickness $h = 0.1$ m, and lengths of 2, 5 and 10 meters. Comparing the results indicates that RKPM can predict the buckling loads with an accuracy of more than 99 percent.

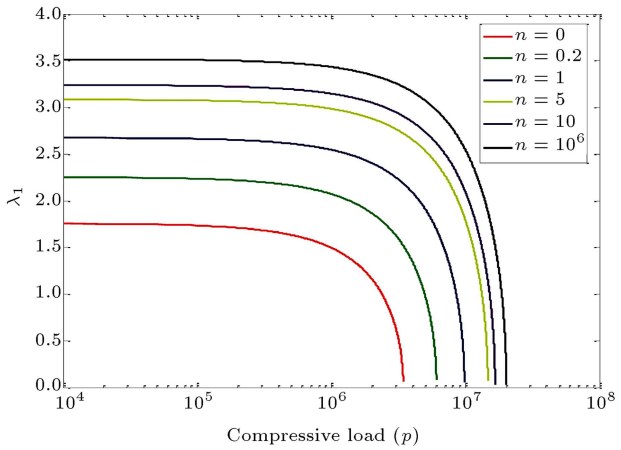

Figure 8. Variation of the first non-dimensional frequency with the compressive load (p) for different material distributions.

Figure 8 shows variations of the first non-dimensional natural frequency of a cantilevered FGM beam versus compressive load, for different material distributions. From Figure 8, it is seen that, as the power exponent increases, critical buckling load also increases. This is due to higher contribution of a ceramic component in the structure. Table 8 represents critical buckling loads of an FGM beam at different beam lengths, material distributions, and boundary conditions, where letters C, F and S stand

Table 8. Critical buckling loads (unit: MN) for FGM beams with different material distributions and end supports.

Length	BC's	$n = 0$	$n = 0.2$	$n = 1$	$n = 5$	$n = 10$	$n = 10^6$
$L = 2$ m	CF	0.688	1.218	1.968	2.944	3.332	4.04
	SS	2.74	4.88	7.88	11.78	13.34	16.17
	CS	5.642	9.988	16.128	24.130	27.298	33.10
	CC	11.042	19.543	31.541	47.203	53.406	64.760
$L = 5$ m	CF	0.1102	0.195	0.315	0.471	0.533	0.646
	SS	0.4412	0.781	1.261	1.887	2.1344	2.586
	CS	0.902	1.598	2.580	3.860	4.366	5.296
	CC	1.766	3.126	5.048	7.554	8.546	10.360
$L = 10$ m	CF	0.0274	0.0486	0.0786	0.1178	0.1332	0.1616
	SS	0.11	0.1952	0.315	0.4716	0.534	0.647
	CS	0.226	0.399	0.645	0.965	1.0918	1.324
	CC	0.442	0.781	1.262	1.888	2.136	2.590

for clamped, simply supported and free boundary conditions.

8. Conclusion

In this paper, free vibration characteristics and buckling loads of functionally graded beams are analyzed. A system of equations of motion is derived using Lagrange's equations, under the assumption of the Euler-Bernoulli beam theory. Boundary conditions are taken into account using Lagrange multipliers. It is assumed that the material properties of the beam vary continuously in the thickness direction according to the power-law form. RKPM is applied to solve the eigenvalue equation of FGM beams. Natural frequencies and buckling loads of the FGM beam are evaluated. For the case where $n \to \infty$, results of natural frequencies and buckling loads are in good agreement with analytical findings. The accuracy of the findings shows that the RKPM technique is a reliable method for analysis of FGM structures, in which the neutral axis is usually displaced and the density of the components is not homogenous. In this study, the effect of material distribution, compressive load and boundary conditions on the vibration characteristics of the beam is discussed. The meshless method of RKPM is shown to be a powerful tool for the vibration analysis and buckling load of beams with non-homogenous material distribution in the thickness direction in which the neutral axis can be displaced drastically.

Nomenclature

A	Area of beam cross section
a	Dilation parameter
b	Width of beam cross section
$b_i(x)$	Coefficients of base functions
b^T	Transposed vector of coefficients of base function
$C(x; x-y)$	Correction function
$C_I(t)$	Degrees of freedom for test functions
$D_I(t)$	Degrees of freedom for trial functions
$E(\tilde{z})$	Young's modulus of the beam
$(EI)_{\text{eq}}$	Equivalent EI
h	Height of beam cross section
$H(x-y)$	Vector of base functions
I	Moment of inertia of beam cross section
K	Stiffness matrix
L, l	Length of beam
$M^{\frown}$	Bending moment of cross section
$M^{\sim}$	Matrix of moments of kernel functions
M	Mass matrix
m	Mass per unit length of beam
$m_k(x)$	Moment of kernel function
n	Power exponent in Eq. (13), order of correction polynomial in Eq. (17)
NP	Total number of particles
p	Compressive axial load
T	Kinetic energy of beam
U	Potential energy of beam
u	Axial displacement
$u^R(x)$	Reproduced function
v	Lateral displacement
w	Transverse displacement
x	Coordinate in axial direction
x_I	Position of Ith particle
Δx_I	Specific length of particle I

z	Distance of an arbitrary point from neutral axis of the beam
$\tilde{z}$	Distance of an arbitrary point from bottom surface of the beam
$\tilde{z}_c$	Position of neutral axis
δ	Variation
ε_{xx}	Normal strain
λ	Non-dimensional natural frequency
$\rho(\tilde{z})$	Density
σ_{xx}	Normal stress
$\{\Phi_i\}$	Vector of mode shapes
ϕ_a	Kernel function
$\overline{\phi}_a$	Corrected kernel function
$\psi_I(x)$	Shape function of particle I
Ω	Domain of integration
ω	Natural frequency

References

1. Suresh, S. and Mortensen, A., *Fundamentals of Functionally Graded Materials*, Cambridge Publication, London (1998).
2. Zhang, X., Li, W., Hong, C., Han, W. and Han, J. "A novel development of ZrB_2/ZrO_2 functionally graded ceramics for ultrahigh-temperature application", *Int. J. of Scripta Materialia*, **59**, pp. 1214-1217 (2008).
3. Cetinel, H., Uyulgan, B., Tekmen, C., Ozdemir, I. and Celik, E. "Wear properties of functionally gradient layers on stainless steel substrates for high temperature applications", *Int. J. of Surface and Coatings Technology*, **174**, pp. 1089-1094 (2003).
4. Gelbstein, Y., Dashevsky, Z., George, Y. and Dariel, M.P. "Development of p-Pb1_xSnxTe functionally graded materials", *Int. J. of Physica*, **391**, pp. 256-265 (2007).
5. Fujihara, K., Gopal, R., Loh, P.L., Ganesh, V.K., Ramakrisshna, S., Foong, K.W. and Chew, C.L. "Fibrous composite materials in dentistry and orthopaedics: review and applications", *Int. J. of Composites Science and Technology*, **64**, pp. 775-788 (2004).
6. Watari, F., Yokoyama, A., Omori, M., Hirai, T., Kondo, H., Uo, M. and Kawasaki, T. "Biocompatibility of materials and development to functionally graded implant for bio-medical application", *Int. J. of Composites Science and Technology*, **64**, pp. 893-908 (2004).
7. Erisken, C., Kaylon, D.M. and Wang, H. "Functionally graded electrospun polycaprolactone and b-tricalcium phosphate nanocomposites for tissue engineering applications", *Int. J. of Biomaterials*, **29**, pp. 4065-4073 (2008).
8. Muller, E., Drasar, C., Schilz, J. and Kaysser, W.A. "Functionally graded materials for sensor and energy applications", *Int. J. of Materials Science and Engineering*, **362**, pp. 17-39 (2003).
9. Bever, M.B. and Duwez, P.E. "Gradients in Composites Materials", *Int. J. of Materials Science and Engineering*, **10**, pp. 1-8 (1972).
10. Chakraborty, A., Gopalakrishnan, S. and Reddy, J.N. "A new beam finite element for the analysis of functionally graded materials", *Int. J. of Mech. Sci.*, **45**, pp. 519-539 (2003).
11. Xiang, H.J. and Yang, J. "Free and forced vibration of a laminated FGM Timoshenko beam of variable thickness under heat conduction", *Int. J. of Composites Part B: Engineering*, **39**, pp. 292-303 (2008).
12. Aydogdu, M. "Semi-inverse method for vibration and buckling of axially functionally graded beams", *Int. J. of Reinforced Plastics and Composites*, **27**, pp. 683-691 (2008).
13. Simsek, M. and Kocaturk, T. "Free and forced vibration of a functionally graded beam subjected to a concentrated moving harmonic load", *Int. J. of Composite Structures*, **90**, pp. 465-473 (2009).
14. Sina, S.A., Navazi, H.M. and Haddadpou, H. "An analytical method for free vibration analysis of functionally graded beams", *Int. J. of Mater. & Des.*, **30**, pp. 741-747 (2009).
15. Simsek, M. "Vibration analysis of a functionally graded beam under a moving mass by using different beam theories", *Int. J. of Composite Structures*, **92**, pp. 904-917 (2010).
16. Alshorbagy, A.E., Eltaher, M.A. and Mahmoud, F.F. "Free vibration characteristics of a functionally graded beam by finite element method", *Int. J. of Applied Mathematical Modeling*, **35**, pp. 412-425 (2011).
17. Rao Singiresu, S., *Vibration of Continuous Systems*, John Wiley & Sons Inc, New Jersey, Hoboken (2007).
18. Rahaeifard, M., Moeini, S.A., Kahrobaiyan, M.H. and Ahmadian, M.T. "Vibration analysis of a rotating FGM cantilever arm", *Proceedings of the ASME 2009 International Mechanical Engineering Congress & Exposition, IMECE-11062*, Florida, USA (2009).
19. Lui, W.K., Chen, Y., Jun, S., Chen, S., Belytschko, T., Pan, C., Uras, R.A. and Chang, C.T. "Overview and application of the reproducing kernel particle methods", *Int. J. of Computational Methods in Engineering*, **3**, pp. 3-80 (1996).
20. Zhou, J.X., Zhang, H.Y. and Zhang, L. "Reproducing kernel particle method for free and forced vibration analysis", *Int. J. of Sound and Vibration*, **279**, pp. 389-402 (2005).
21. Lu, Y.Y., Belytschko, T. and Gu, L. "A new implementation of the element free Galerkin method", *Int. J. of Comput. Methods Appl. Mech. Engrg.*, **113**, pp. 397-414 (1994).
22. Rao Singiresu, S., *Mechanical Vibrations*, Pearson Education, Inc., 5th Edition, Chapter 8, pp. 733-734, Prentice Hall, New Jersey, USA (2011).

23. Timoshenko, S. and Young, D.H., *Vibration Problems in Engineering*, Van Nostrand Company, New York, USA (1955).

Biographies

Reza Saljooghi received his BS degree in Mechanical Engineering, in 2008, from Iran University of Science and Technology, Tehran, Iran, and his MS degree in Mechanical Engineering, Applied Design, at Sharif University of Technology, Tehran, Iran, in 2011. He is now junior lecturer at Hormozgan University, Iran, and his research interests include active vibration control of FGMs and smart structures, hybrid vehicles' dynamics and vibration, active and semi active suspension systems and MEMS/NEMS.

Mohammad Taghi Ahmadian received his BS and MS degrees in Physics, in 1970 and 1972, respectively, from Shiraz University, Shiraz, Iran. He also received his MS degree, in Mechanical Engineering, in 1980, from the University of Kansas in Lawrence, USA, where he also completed PhD degrees in Physics and Mechanical Engineering, in 1980 and 1986, respectively. He is currently Professor in the School of Mechanical Engineering at Sharif University of Technology, Tehran, Iran, and Head of the Bio-Engineering Center. His research interests include micro and nano mechanics, and bioengineering.

Gholam Hossein Farrahi received his PhD degree in Mechanical Engineering, in 1985, from (ENSAM), Paris, France. He is currently Professor in the School of Mechanical Engineering at Sharif University of Technology, Tehran, Iran. He is also Head of the Applied Design Group and the Materials Life Estimation and Improvement Laboratory. His research interests include fatigue, fracture mechanics, shot peening, residual stresses, life improvement methods and failure analysis.